

Proapoptotic BAX and BAK: A Requisite Gateway to Mitochondrial Dysfunction and Death

Michael C. Wei,^{1,2*} Wei-Xing Zong,^{3*} Emily H. -Y. Cheng,¹
Tullia Lindsten,³ Vily Panoutsakopoulou,¹ Andrea J. Ross,⁴
Kevin A. Roth,⁵ Grant R. MacGregor,⁴ Craig B. Thompson,^{3†}
Stanley J. Korsmeyer^{1†}

Multiple death signals influence mitochondria during apoptosis, yet the critical initiating event for mitochondrial dysfunction *in vivo* has been unclear. tBID, the caspase-activated form of a "BH3-domain-only" BCL-2 family member, triggers the homooligomerization of "multidomain" conserved proapoptotic family members BAK or BAX, resulting in the release of cytochrome c from mitochondria. We find that cells lacking both *Bax* and *Bak*, but not cells lacking only one of these components, are completely resistant to tBID-induced cytochrome c release and apoptosis. Moreover, doubly deficient cells are resistant to multiple apoptotic stimuli that act through disruption of mitochondrial function: staurosporine, ultraviolet radiation, growth factor deprivation, etoposide, and the endoplasmic reticulum stress stimuli thapsigargin and thapsigargin. Thus, activation of a "multidomain" proapoptotic member, BAX or BAK, appears to be an essential gateway to mitochondrial dysfunction required for cell death in response to diverse stimuli.

Members of the "BH3-domain-only" subset of BCL-2 family proteins connect proximal death signals to the core apoptotic pathway (1–5). After activation of CD95 (Fas) or TNFR1 death receptors, BID is cleaved and activated to p15 tBID (6–8), which, in a model system using purified mitochondria, serves as a death ligand that induces the oligomerization of BAK (9) and BAX (10). tBID does not cause release of cytochrome c from purified *Bak*-deficient mitochondria, suggesting that interaction of tBID and BAK is a critical event at least *in vitro* (9).

Here we assess whether BAK is required for tBID-induced apoptosis of intact, whole cells by using a retroviral vector to express tBID in murine embryonic fibroblasts (MEFs). Numerous cells with shrunken, apoptotic morphology were detected in *Bak*-deficient as well as wild-type MEFs 24 hours after infection with the

tBID-expressing vector (Fig. 1A), but not with empty vector (pMIG) (11) expressing only green fluorescence protein (GFP). MEFs deficient for BAX, another "multidomain" proapoptotic BCL-2 member, were also killed. In contrast, *Bax*, *Bak* doubly deficient MEFs proved completely resistant to tBID-induced cell death as assessed by multiple markers including Annexin-V staining (Fig. 1C) and cell morphology (Fig. 1A). Infected cells could be identified by expression of GFP (Fig. 1B) and revealed a similar infection rate by control pMIG virus in all genetic backgrounds (Fig. 1D). Analysis of GFP expression in tBID-infected MEFs revealed small amounts of GFP in apoptotic cells of wild-type, *Bax*^{-/-}, and *Bak*^{-/-} MEFs (Fig. 1D). In contrast, introduction of the tBID vector into *Bax*, *Bak* doubly knocked out (DKO) MEFs revealed cells with normal morphology expressing high levels of GFP (Fig. 1, B and D). Simian virus 40 (SV40)-transformed MEF cell lines of wild-type and DKO genotypes also proved sensitive and resistant to tBID, respectively (12). Protein immunoblotting confirmed expression of p15 BID in DKO MEFs and smaller amounts in wild-type MEFs undergoing apoptosis (Fig. 1E). p15 BID localized to the mitochondria as an integral membrane protein in both wild-type and DKO MEFs (12), indicating that although tBID was expressed and targeted to mitochondria, it did not kill DKO MEFs. Reexpression of BAX alone was not sufficient to kill DKO MEFs but did restore killing by tBID, confirming tBID's require-

ment for a multidomain proapoptotic member to induce apoptosis (Fig. 1C).

One mechanism to account for these observations would be if tBID induced the activation of BAX and BAK, resulting in mitochondrial dysfunction including the release of cytochrome c. We tested the activation status of BAX and BAK and the intracellular distribution of cytochrome c in primary MEFs expressing tBID. Mitochondria from control and p15 BID-expressing primary MEFs were treated with the chemical cross-linker bismaleimido-hexane (BMH) to examine the status of BAK oligomerization. As we observed in hepatocytes (9), the faster migrating inactive BAK conformer in control cells disappeared in cells expressing p15 BID, and there was a corresponding increase in the amount of cross-linked BAK multimers consistent with formation of dimers and trimers (Fig. 2A). This process appeared to be independent of BAX, as p15 BID caused oligomerization of BAK in *Bax*^{-/-} MEFs (Fig. 2A). Expression of p15 BID in wild-type MEFs caused cytosolic BAX to translocate and insert as an integral mitochondrial membrane protein (12), as BAX does in Fas-activated hepatocytes (Fig. 3B). In GFP-positive, tBID-expressing DKO MEFs, cytochrome c remained in a punctate mitochondrial pattern, but in tBID-expressing wild-type MEFs, cytochrome c redistributed to a diffuse cytosolic pattern (Fig. 2B). Thus, activation of proapoptotic BAX, BAK, or both is required for tBID-induced cytochrome c release *in vivo*. We tested whether *Bax/Bak*-deficient cells had an intact apoptotic pathway downstream of mitochondria by microinjecting cytochrome c into the cytoplasm of MEFs. DKO and wild-type MEFs showed comparable cell death after microinjection of cytochrome c (Fig. 2C), indicating that the apoptotic pathway downstream of cytochrome c release (13) does not depend on function of BAX or BAK.

To examine whether BAK or BAX molecules are required for cell deaths *in situ*, we assessed apoptosis in the livers of mice injected with agonistic antibody to Fas. *Bak*-deficient mice were susceptible to Fas-induced hepatocellular apoptosis and hemorrhagic necrosis

Table 1. Susceptibility of mice lacking *Bax*, *Bak*, or both to anti-Fas injection. Mice were injected intravenously with 0.5 μ g of monoclonal antibody to Fas (Jo2, Pharmingen) per gram of body weight and killed when moribund or observed for up to 24 hours. Mean survival time in hours \pm 1 SD is shown for mice that died.

Genotype	Dead/ injected	Mean survival (hours)
<i>Bak</i> ^{-/-}	9/13	5.2 \pm 1.7
<i>Bax</i> ^{+/-} or <i>+/+</i>	9/14	6.0 \pm 2.7
<i>Bax</i> ^{-/-}	7/10	3.8 \pm 1.2
<i>Bax</i> ^{+/-} or <i>+/+</i>	13/13	2.6 \pm 1.9
<i>Bax</i> ^{-/-} , <i>Bak</i> ^{-/-}	0/3	(killed after 9 hours)

¹Howard Hughes Medical Institute, Departments of Pathology and Medicine, Harvard Medical School, Dana-Farber Cancer Institute, Boston, MA 02115, USA. ²Division of Biology and Biomedical Sciences, Washington University School of Medicine, St. Louis, MO 63110, USA. ³Departments of Medicine and Pathology and Laboratory Medicine, Abramson Family Cancer Research Institute, University of Pennsylvania, Philadelphia, PA 19104, USA. ⁴Center for Molecular Medicine, Emory University School of Medicine, Atlanta, GA 30322, USA. ⁵Department of Pathology, Washington University School of Medicine, St. Louis, MO 63110, USA.

*These authors contributed equally to this work.
†To whom correspondence should be addressed. E-mail: craig@mail.med.upem.edu; stanley_korsmeyer@dfci.harvard.edu

REPORTS

(Fig. 3A and Table 1), dying in a similar time course to that of wild-type or heterozygous littermate controls. This contrasts with the resistance to Fas of *Bid*-deficient mice (14). Subcellular fractionation of hepatocytes activated through Fas in vivo revealed that BAX translocates from cytosol to mitochondria in *Bak*-deficient, but not *Bid*-deficient mice (Fig. 3B). *Bax*-deficient mice also succumbed to Fas-induced hepatocellular apoptosis (Fig. 3A and Table 1). Thus, BID appears to function upstream of both BAX and BAK in hepatocytes as well as in MEFs.

We next tested whether elimination of both BAX and BAK would confer resistance to Fas-induced hepatocellular apoptosis. The vast majority of *Bax*, *Bak* DKO mice die around the time of birth, and only a small percentage survive to adulthood (15). We injected the three

available DKO mice with antibody to Fas, all of which survived 9 hours, at which time they were killed and their livers were examined (Table 1). The DKO mice displayed at most moderate apoptosis of hepatocytes, and some animals showed none (Fig. 3A). The immunohistochemistry profile of affected DKO hepatocytes was limited to focal areas of Caspase-3 activation without release of cytochrome c (Fig. 3C), similar to that seen in *Bid*^{-/-} hepatocytes (14). These data on the limited number of DKO mice available contrasted with those from the singly deficient mice, indicating that BID-dependent apoptosis also used either BAX or BAK in hepatocytes. This illustrates that “extrinsic” (death receptor) paths, when activated in situ, may also depend on “multidomain” proapoptotic proteins in select cell types (14, 16).

We next examined whether BAX, BAK, or

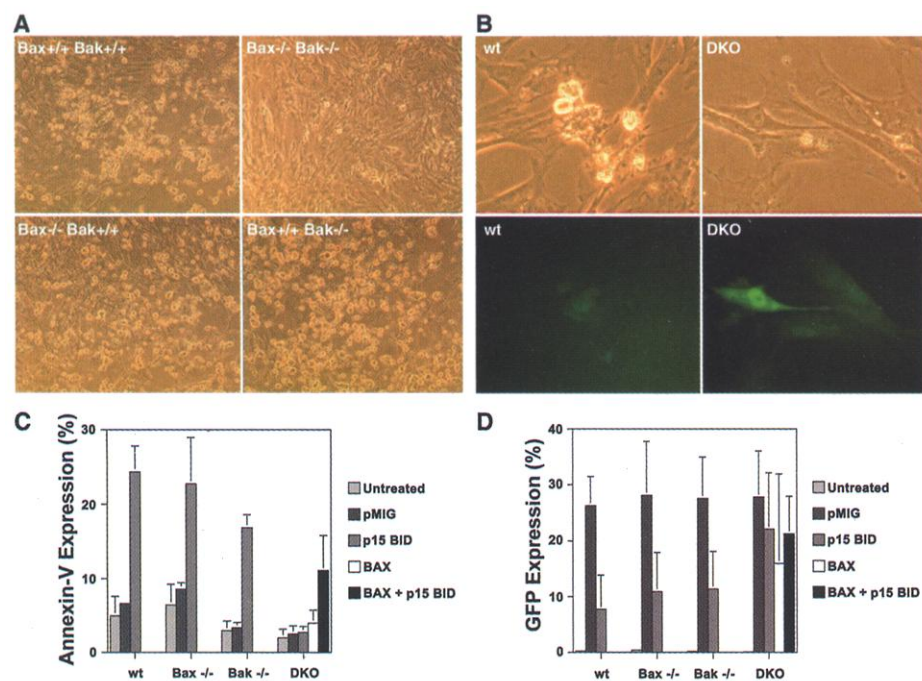


Fig. 1. Resistance of *Bax*, *Bak* doubly deficient murine embryonic fibroblasts (MEFs) to tBID-induced apoptosis. (A) Bright-field microscopy ($\times 20$ magnification) of wild-type, *Bax*^{-/-} *Bak*^{-/-}, *Bax*^{-/-} *Bak*^{+/+}, and *Bax*^{+/+} *Bak*^{-/-} primary embryonic day 13.5 MEFs 24 hours after infection with a tBID-expressing vector. Murine p15 BID and BAX were cloned into the retroviral expression vector MSCV-IRES-GFP (pMIG) (71). Retroviruses were generated by transfecting 293GPG packaging cell line as described (33). Retrovirus-containing supernatant was collected 3 and 5 days after transfection and used to infect MEFs in the presence of polybrene (8 μ g/ml). (B) Bright-field and GFP fluorescence of the same field ($\times 40$ magnification) of wild-type (wt) and DKO MEFs 24 hours after infection with the tBID vector. (C) Quantitation of apoptosis in MEFs shown at the 24-hour time point after infection with pMIG (empty vector control), tBID, and/or BAX vectors. Cell death was quantitated by flow cytometric detection of Annexin-V staining (Bio-vision). Values shown are mean \pm 1 SD from three independent experiments. (D) Quantitation of GFP-positive cells 24 hours after infection with pMIG, tBID, and/or BAX vectors. GFP-positive cells were detected by flow cytometry. Values shown are mean \pm 1 SD from three independent experiments. (E) Immunoblot with antibody to Bid of whole-cell lysates from SV40-transformed (34) wild-type and DKO MEFs at 17 hours after infection with pMIG or tBID vectors.

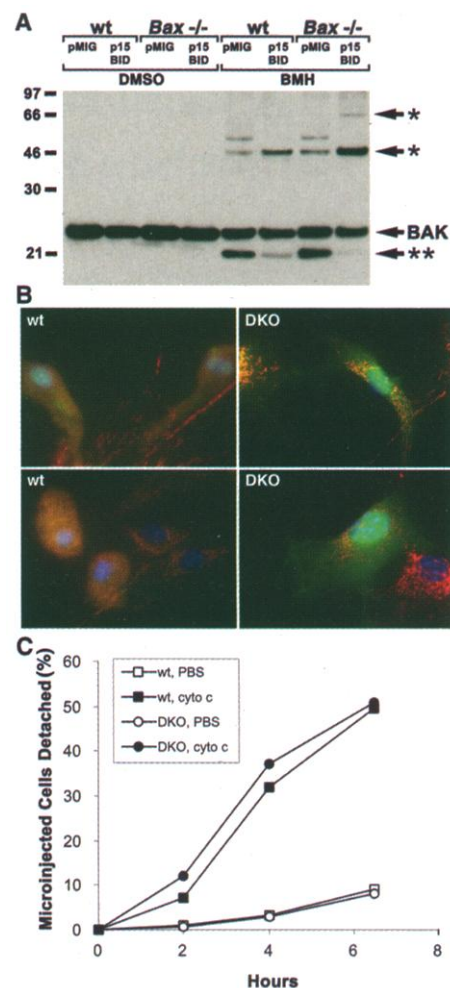


Fig. 2. Function of BAX and BAK downstream of tBID and upstream of cytochrome c release. (A) tBID-induced BAK oligomerization independent of BAX. Mitochondria-enriched fractions from pMIG or tBID vector-infected MEFs were prepared as described (14) and treated with dimethyl sulfoxide (DMSO) containing control buffer or 10 mM BMH cross linker (Pierce). Cross-linked BAK species were detected by antibody to BAK (Upstate Biotechnology) immunoblot. * indicates BAK complexes consistent with dimers or trimers; ** indicates inactive BAK conformer. (B) Cytochrome c release in DKO MEFs. Three-color fluorescence microscopy (35) of wild-type and DKO MEFs at 24 hours after infection with tBID and GFP-expressing vector. Red indicates cytochrome c immunostaining. Blue is Hoechst staining of DNA. Green is GFP expression in infected cells. Overlap of GFP and cytochrome c staining is denoted by yellow. Results are representative of three independent experiments. (C) Apoptosis of DKO MEFs after microinjection of cytochrome c. Primary MEFs were plated on 1% gelatin-coated gridded cover slips. Purified cytochrome c (1.6 mg/ml) dissolved in phosphate-buffered saline (PBS) or PBS control was mixed 1:1 with 0.5% fluorescein isothiocyanate-conjugated dextran and microinjected into cells with an Eppendorf 5246 Transjector at a pressure of 150 hPa and an injection time of 0.5 s. Apoptotic cells detach from the cover slip and were counted as a measure of apoptosis, enabling a time course of the mean percentages of microinjected cells that detach to be plotted from three independent experiments.

REPORTS

both were required for death after other stimuli proposed to cause cytochrome c release from mitochondria (17–21). Wild-type, *Bax*^{-/-}, and *Bak*^{-/-} MEFs were susceptible, whereas DKO MEFs proved resistant to staurosporine (kinase inhibitor), etoposide (topoisomerase II inhibitor), and ultraviolet radiation (UVC), even at very high doses (Fig. 4, A to D). Time course studies as well as dose response evaluations indicated that DKO MEFs are markedly resistant to these stimuli, demonstrating long-term survival when assessed by nucleosomal DNA fragmentation (Fig. 4A), dye exclusion (Fig. 4D), or Annexin-V staining (Fig. 4E). Moreover, DKO MEFs, but not singly deficient MEFs, proved resistant to stress signaling from the endoplasmic reticulum (ER) (22–24) induced by thapsigargin (which inhibits the Ca²⁺ adenosine triphosphatase pump), tunicamycin (which inhibits N-linked glycosylation) (Fig. 4B), or brefeldin A (which inhibits ER-Golgi

transport) (12). Further assessment indicated that postmitochondrial events were prevented in DKO cells, including the activation of effector caspase activity after all of these stimuli (Fig. 4C). DKO MEFs were also resistant to cell death caused by serum (growth factor) deprivation (Fig. 4F). In contrast, *Bid*^{-/-} cells were susceptible to all of these signals (Fig. 4, A and B), indicating that they are not dependent on BID and that BID is not the sole activator of BAX or BAK. DKO MEFs were susceptible to the extrinsic signal of tumor necrosis factor α (TNF- α) plus actinomycin D, which in this cell type induces a mitochondria-independent caspase cascade (Fig. 4, A and C). Considerable uncertainty has existed as to

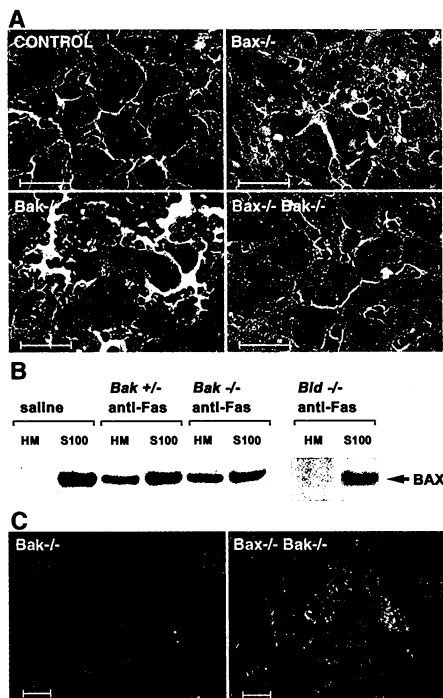


Fig. 3. Function of BAX and BAK downstream of BID in Fas-induced hepatocellular apoptosis. (A) Hematoxylin and eosin-stained liver sections from *Bak*^{-/-}, *Bax*^{-/-}, and DKO mice treated with antibody to Fas (anti-Fas). Bar represents 20 μ m. (B) Fas-induced BAX translocation from cytosol to mitochondria in hepatocytes is downstream of BID but independent of BAK. BAX immunoblot of mitochondrial (HM) and cytosolic (S100) fractions of hepatocytes prepared as previously described (8) from wild-type, *Bid*^{-/-}, *Bak*^{+/-}, and *Bak*^{-/-} mice treated with saline or anti-Fas. (C) Three-color immunohistochemistry of livers from anti-Fas-treated *Bak*^{-/-} and DKO mice. Cytochrome c staining is in green, activated Caspase-3/7 (CM1 antibody) in red, and nuclei stained with Hoechst in blue. Bar represents 20 μ m. Histology and immunohistochemical staining of livers from anti-Fas-treated animals were done as described (14).

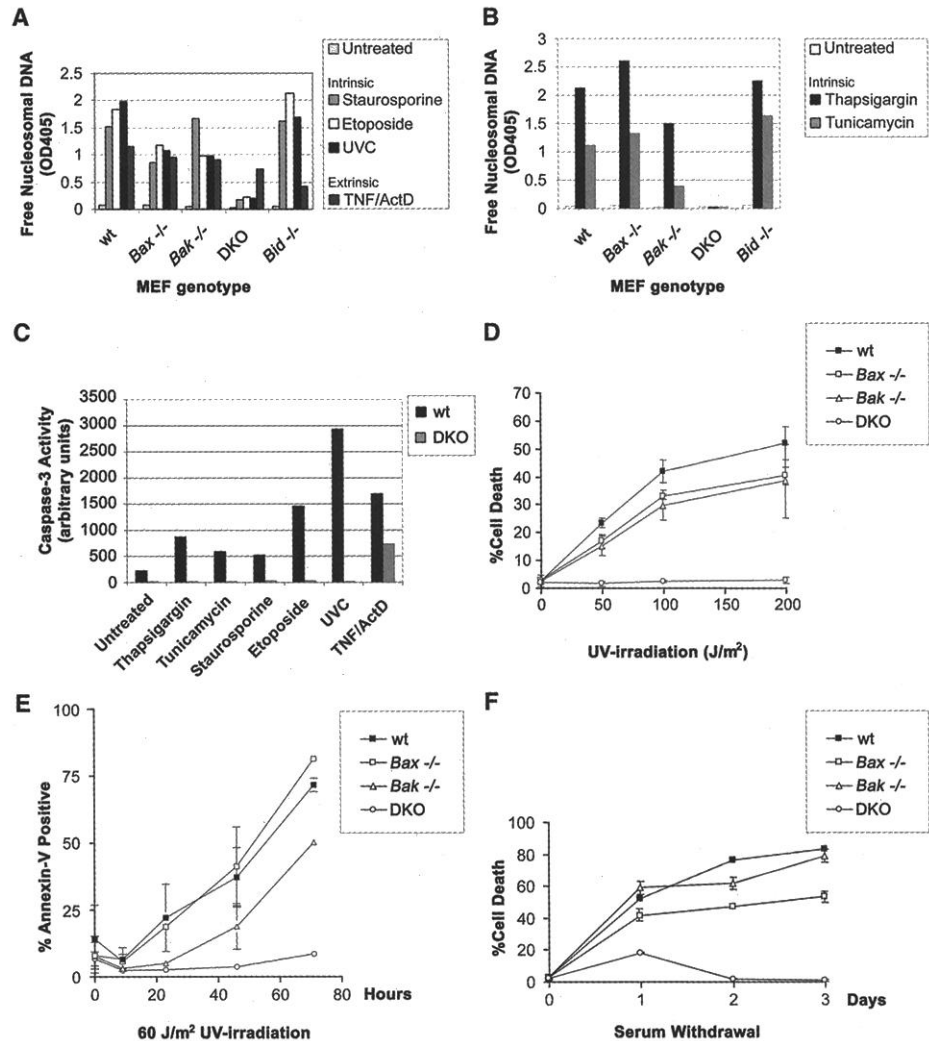


Fig. 4. Resistance of *Bax*, *Bak* doubly deficient MEFs to multiple intrinsic death signals. (A) Susceptibility of MEFs to apoptotic death by mitochondria-dependent intrinsic signals. Wild-type, *Bax*^{-/-}, *Bak*^{-/-}, DKO, and *Bid*^{-/-} primary MEFs were treated with 1 μ M staurosporine, 100 μ M etoposide, UVC (60 J/m²), or TNF- α (1 ng/ml) + actinomycin D (2 μ g/ml), and a 48-hour time point is shown. Average values from duplicate samples of an enzyme-linked immunosorbent assay of apoptotic DNA fragmentation (Roche) are plotted as representative of three independent experiments. (B) Susceptibility of MEFs to apoptotic death by ER stimuli. As in (A), genotyped MEFs were treated with 2 μ M thapsigargin or tunicamycin (1 μ g/ml), and average values from duplicate samples at a 48-hour time point of apoptotic DNA fragmentation were plotted. DKO MEFs also demonstrated long-term survival when assessed by Annexin-V staining 4 days after the stimuli (12). (C) Quantitation of effector caspase activity (e.g., Caspase-3) using DEVD-AFC fluorogenic substrate (Clontech). Wild-type and DKO MEFs were treated with the following death signals and harvested at indicated time points: 2 μ M thapsigargin (36 hours), tunicamycin (1 μ g/ml; 36 hours), 1 μ M staurosporine (16 hours), 100 μ M etoposide (24 hours), UVC (60 J/m²; 24 hours), and TNF- α (1 ng/ml) + actinomycin D (2 μ g/ml; 16 hours). Results are representative of three independent experiments. (D) Dose response of MEFs to UVC irradiation. Cell death was quantitated by trypan blue exclusion, and a 24-hour time point was plotted. (E) Time course of MEF apoptosis after exposure to UVC (60 J/m²). Cell death was quantitated by flow cytometric detection of Annexin-V staining. Long-term survival of DKO MEFs was also noted 4 days after staurosporine and etoposide, as well as UVC treatments (12). (F) Time course of MEF apoptosis in response to serum withdrawal. Cell death was quantitated by trypan blue exclusion.

whether anti- or proapoptotic BCL-2 members exert a dominant role. Our studies indicate that in vivo, intact cells require a multidomain proapoptotic member to respond to a diverse set of death signals. tBID must activate BAX or BAK to initiate mitochondrial dysfunction and cell death in hepatocytes and MEFs. Conceivably, in other tissues, this function may be served by other proapoptotic multidomain family members such as BOK (25). Activation and oligomerization of BAX or BAK have been proposed to result in formation of a homomultimeric pore (9, 26), formation of a voltage-dependent anion channel-containing pore (27), or permeabilization of mitochondrial membranes (28) to initiate cytochrome c release. Release of cytochrome c activates the Apaf-1-Caspase-9 apoptosome and downstream effector caspases (13), and after substantial loss of cytochrome c, progressive caspase-independent mitochondrial dysfunction can lead to cell death (29). Knockouts of cytochrome c or Caspase-9 and Apaf-1, which function downstream of mitochondria, indicate that damage from staurosporine, etoposide, and radiation depends on signals mediated by cytochrome c release from mitochondria (17–21). The *Bax*, *Bak*-deficient cells, which have a block immediately upstream of mitochondria, appear even better protected from these agents. Even ER stress-induced apoptosis requires BAX or BAK, which might reflect undefined roles of BAX or BAK at ER sites (30, 31) or an ultimate dependence of ER pathways on mitochondria (32). Other upstream activators of BAX and BAK clearly exist, as *Bid*-deficient cells are often susceptible to stimuli that fail to kill cells lacking both BAX and BAK. Our loss-of-function studies reveal that the absence of proapoptotic BAX and BAK molecules creates a profound block, preserving mitochondria and inhibiting apoptosis after seemingly unrelated signals initiated at multiple sites including plasma membrane, nucleus, and ER.

References and Notes

1. D. R. Green, *Cell* **102**, 1 (2000).
2. G. Kroemer, J. C. Reed, *Nature Med.* **6**, 513 (2000).
3. J. M. Adams, S. Cory, *Science* **281**, 1322 (1998).
4. A. Gross, J. M. McDonnell, S. J. Korsmeyer, *Genes Dev.* **13**, 1899 (1999).
5. D. C. Huang, A. Strasser, *Cell* **103**, 839 (2000).
6. H. Li, H. Zhu, C. J. Xu, J. Yuan, *Cell* **94**, 491 (1998).
7. X. Luo, I. Budihardjo, H. Zou, C. Slaughter, X. Wang, *Cell* **94**, 481 (1998).
8. A. Gross et al., *J. Biol. Chem.* **274**, 1156 (1999).
9. M. C. Wei et al., *Genes Dev.* **14**, 2060 (2000).
10. R. Eskes, S. Desagher, B. Antonsson, J. C. Martinou, *Mol. Cell Biol.* **20**, 929 (2000).
11. L. Van Parijs et al., *Immunity* **11**, 281 (1999).
12. M. C. Wei, W.-X. Zong, unpublished data.
13. P. Li et al., *Cell* **91**, 479 (1997).
14. X. M. Yin et al., *Nature* **400**, 886 (1999).
15. T. Lindsten et al., *Mol. Cell* **6**, 1389 (2000).
16. C. Scaffidi et al., *EMBO J.* **17**, 1675 (1998).
17. R. Hakem et al., *Cell* **94**, 339 (1998).
18. K. Kuida et al., *Cell* **94**, 325 (1998).
19. H. Yoshida et al., *Cell* **94**, 739 (1998).
20. F. Cecconi, G. Alvarez-Bolado, B. I. Meyer, K. A. Roth, P. Gruss, *Cell* **94**, 727 (1998).
21. K. Li et al., *Cell* **101**, 389 (2000).

22. R. J. Kaufman, *Genes Dev.* **13**, 1211 (1999).
23. T. Nakagawa et al., *Nature* **403**, 98 (2000).
24. H. He, M. Lam, T. S. McCormick, C. W. Distelhorst, *J. Cell Biol.* **138**, 1219 (1997).
25. S. Y. Hsu, A. Kaipia, E. McGee, M. Lomeli, A. J. Hsueh, *Proc. Natl. Acad. Sci. U.S.A.* **94**, 12401 (1997).
26. M. Saito, S. J. Korsmeyer, P. H. Schlesinger, *Nature Cell Biol.* **2**, 553 (2000).
27. S. Shimizu, M. Narita, Y. Tsujimoto, *Nature* **399**, 483 (1999).
28. R. M. Kluck et al., *J. Cell Biol.* **147**, 809 (1999).
29. V. K. Mootha et al., *EMBO J.* **20**, 661 (2001).
30. W. Zhu et al., *EMBO J.* **15**, 4130 (1996).
31. F. W. Ng et al., *J. Cell Biol.* **139**, 327 (1997).
32. J. Hacki et al., *Oncogene* **19**, 2286 (2000).
33. D. S. Ory, B. A. Neugeboren, R. C. Mulligan, *Proc. Natl. Acad. Sci. U.S.A.* **93**, 11400 (1996).
34. Primary murine embryonic fibroblasts were generated from *Bax*^{+/-};*Bak*^{+/-} or *Bax*^{+/-};*Bak*^{-/-} timed matings at 13.5 days after conception. Primary MEFs were immortalized by transfection with a plasmid containing SV40 genomic DNA. Primary MEFs were plated in six-well plates and were transfected with 1 μg of total DNA using Fugene (Roche) according to

the manufacturer's instructions. Stable immortalized clones were generated through serial dilution.

35. Cells were fixed in 3% paraformaldehyde and permeabilized in 1% bovine serum albumin and 0.1% Triton X-100. Cells were sequentially incubated with primary antibody to cytochrome c (clone 6H2.B4, Pharmingen) and Cy3-conjugated goat secondary antibody to mouse (Jackson ImmunoResearch Laboratories) and Hoechst 33258 (Molecular Probes) and then mounted under a cover slip with *N*-propyl gallate. Images were acquired with a SPOT camera (Diagnostics) mounted on Nikon Eclipse E600 with PlanFluor objectives or Olympus IX50 microscopes.
36. We thank E. Smith for figure and manuscript preparation, B. Avery and S. Wade for animal husbandry, C. Gramm for technical assistance, C. Beard for assistance with retrovirus, P. Tegtmeyer for SV40 expression vector, and W. Sellers for use of the microinjector. M.C.W. is supported in part by NIH training grant 5T32AT09361. W.-X.Z. is supported by a postdoctoral grant from the Cancer Research Institute. This work is supported in part by NIH grants R01CA50239 and R37CA48023.

17 January 2001; accepted 29 March 2001

Allosteric Control of RNA Polymerase by a Site That Contacts Nascent RNA Hairpins

Innokenti Touloukhonov,*† Irina Artsimovitch,* Robert Landick‡

DNA, RNA, and regulatory molecules control gene expression through interactions with RNA polymerase (RNAP). We show that a short α helix at the tip of the flaplike domain that covers the RNA exit channel of RNAP contacts a nascent RNA stem-loop structure (hairpin) that inhibits transcription, and that this flap-tip helix is required for activity of the regulatory protein NusA. Protein-RNA cross-linking, molecular modeling, and effects of alterations in RNAP and RNA all suggest that a tripartite interaction of RNAP, NusA, and the hairpin inhibits nucleotide addition in the active site, which is located 65 angstroms away. These findings favor an allosteric model for regulation of transcript elongation.

Evolutionarily conserved, multisubunit RNAPs transcribe genes into RNAs in all known organisms. A universal feature of these RNAPs is a regulated conversion from an initiating form that holds the RNA weakly, to an elongating form that holds RNA tightly during RNA synthesis, and then back to a terminating form that releases RNA. The molecular basis of this switch is unknown. However, conservation from bacteria to humans of RNAP's core subunit composition (β' $\beta\alpha_2$ in bacteria), amino acid sequences, three-dimensional structure, and contacts to DNA and RNA suggest that the switch will be similar for all multisubunit RNAPs (1–3).

A nascent RNA hairpin can terminate tran-

scription by bacterial RNAP if the hairpin includes the 3 to 5 nucleotides (nt) usually found in the RNA exit channel and disrupts at least 1 base pair (bp) of the \sim 8-bp nascent RNA: template DNA hybrid that is present in stable transcription elongation complexes (TECs) (4–7). Similar RNA hairpins can also pause, rather than terminate, transcription when they form more upstream but near the RNA:DNA hybrid, rather than invade it. Both hairpin-dependent pausing and termination can be enhanced by the universal bacterial protein NusA (8, 9).

Two models can explain hairpin effects on transcription (3, 7, 10–15). In the rigid-body model, a pause or terminator hairpin begins forming when only its loop and upper stem have emerged from the exit channel, and then pulls RNA through the channel and away from the active site to avoid steric clash with a rigid RNAP as the lower stem pairs. This partially unwinds the RNA:DNA hybrid and moves RNAP forward without nucleotide addition [the hybrid is wedged against the upstream edge of the active-site cleft in a TEC; see fig. 4A in

Department of Bacteriology, University of Wisconsin, Madison, WI 53706, USA.

*These authors contributed equally to this work.
 †On leave from the Limnological Institute, Russian Academy of Sciences, Irkutsk, Russia.
 ‡To whom correspondence should be addressed. E-mail: landick@bact.wisc.edu